

3D Motor Simulation using Low Pass Filters and Magnitude Response Measures



Veljko Crnadak
School of Electrical Engineering
University of Belgrade, Bulevar kralja Aleksandra 73, 11120
Belgrade, Serbia and Company for Microwave and Millimeter-Wave Techniques and Electronics IMTEL- Komunikacije
Joint-Stock Company Belgrade, Bulevar Mihajla Pupina 165b, 11070
Novi Beograd, Serbia
veljko@insimtel.com

Sinisa Tasic
Company for Microwave Millimeter Wave Techniques and Electronics IMTEL- Komunikacije Joint-Stock Company Belgrade,
Bulevar Mihajla Pupina 165b, 11070 Novi
Beograd, Serbia
tasa@insimtel.com

ABSTRACT: *Using the lumped elements, we have prepared the design of the Chebyshev low pass filter. When the filter with magnitude response is applied, a ladder network with inductor series for shunt capacitors is generated. Initially, we transformed the low pass filter with real lossy reactive elements and then simulated the 3D EM simulator. To experiment with the design created, we simulated the filter obtained the values for S-parameters and compared them. In a frequency value of < 200 MHz, the low pass filter is found to have minimal insertion loss. The filter aims to limit the harmonics during high amplifier output.*

Keywords: Capacitor, Chebyshev, Coil, Filter, Inductor, Low Pass, Lumped, VHF

Received: 28 January 2023, Revised 11 March 2023, Accepted 23 March 2023

DOI: 10.6025/tmd/2023/11/2/43-52

Copyright: with Author

1. Introduction

The magnitude square of the Chebyshev low pass filter transfer function of the N^{th} order is,

$$|H(j\omega)|^2 = \frac{H_0}{1 + \varepsilon^2 T_N^2\left(\frac{\omega}{\omega_c}\right)}, \quad (1)$$

where H_0 is the *dc* attenuation, ε is the ripple magnitude, ω_c is the cutoff frequency and $T_N\left(\frac{\omega}{\omega_c}\right)$ is the Chebyshev polynomial of the N^{th} order,

$$T_N\left(\frac{\omega}{\omega_c}\right) = \begin{cases} \cos\left[N \cos^{-1}\left(\frac{\omega}{\omega_c}\right)\right], & 0 \leq \omega \leq \omega_c \\ \cosh\left[N \cosh^{-1}\left(\frac{\omega}{\omega_c}\right)\right], & \omega > \omega_c \end{cases}. \quad (2)$$

The Chebyshev response, shown in Figure 1, oscillates in the passband between the two values, H_0 and $\frac{H_0}{1 + \varepsilon^2}$, while in the stopband it approaches zero at infinity. The Chebyshev low pass filter is also known as all pole filter, because the transfer function has zeros only at infinity [1]. The poles of the transfer function are all on the left half of the s-plane, and are given with the following expression,

$$s_k = \omega_c(\sigma_k + j\omega_k), \quad k = 1, 2, \dots, N, \quad (3)$$

where

$$\sigma_k = -\sinh\left[\frac{1}{N} \sinh^{-1}\left(\frac{1}{\varepsilon}\right)\right] \sin\frac{(2k-1)\pi}{2N}, \quad (4)$$

and

$$\omega_k = \cosh\left[\frac{1}{N} \sinh^{-1}\left(\frac{1}{\varepsilon}\right)\right] \cos\frac{(2k-1)\pi}{2N}. \quad (5)$$

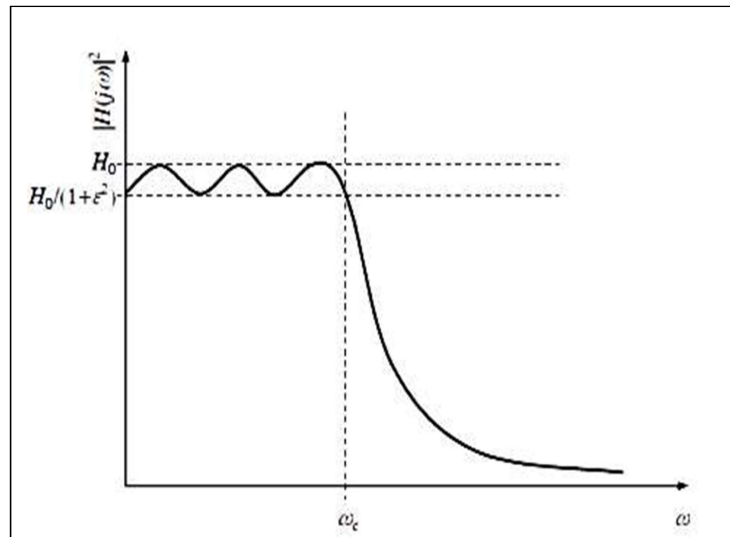


Figure 1. The Chebyshev low pass response of the 6th order [1]

2. Design Theory

Our objective is to design a low pass Chebyshev filter that has a passband ripple of $A = 10 \log(1 + \varepsilon^2) = 0.02$ dB, the cutoff frequency of $f_c = 220$ MHz and an insertion loss at $f = 300$ MHz of at least $L = 35$ dB. Number of reactive elements in the filter is determined from the following inequality,

$$N \geq \frac{\cosh^{-1} \sqrt{\frac{10^{0.1L-1}}{10^{0.1A-1}}}}{\cosh^{-1}\left(\frac{f}{f_c}\right)} \quad (6)$$

From the inequality (6), we learn that the filter has to be of the 9th order at least. Because the source and the load resistance are of 50Ω. each, Figure 2, the dc attenuation of the filter is $H_0 = 1$. Before determining the values of the ideal reactive elements of the circuit in Figure 2, we must obtain the values of the elements of the Chebyshev low pass prototype. The values of the prototype inductances are, $g_1 = g_9 = 0.9021$, $g_3 = g_7 = 1.88$ and $g_5 = 1.972$, the values of the prototype capacitances are, $g_2 = g_8 = 1.4518$ and $g_4 = g_6 = 1.7053$, and the values of the prototype resistances are, $g_0 = g_{10} = 1$. The values of the prototype elements were obtained using the recursion formulas [2].

The actual values of the filter inductances are,

$$L_k = \frac{R_0 g_{(2k-1)}}{\omega_c}, k = 1, 2, 3, \quad (7)$$

and the actual values of the filter capacitances are,

$$C_k = \frac{g_{2k}}{R_0 \omega_c}, k = 1, 2, \quad (8)$$

where $R_0 = 50\Omega$ and $\omega_c = 2\pi f_c$.

We see from the formula (7), that there are three different inductances in the filter, as it is shown in Figure 2, $L_1 = 32.63$ nH, $L_2 = 68.0026$ nH and $L_3 = 71.3123$ nH.

We see from the expression (8), that there are two different capacitances in the filter, as it is shown in Figure 2, $C_1 = 21.0056$ pF and $C_2 = 24.6733$ pF.

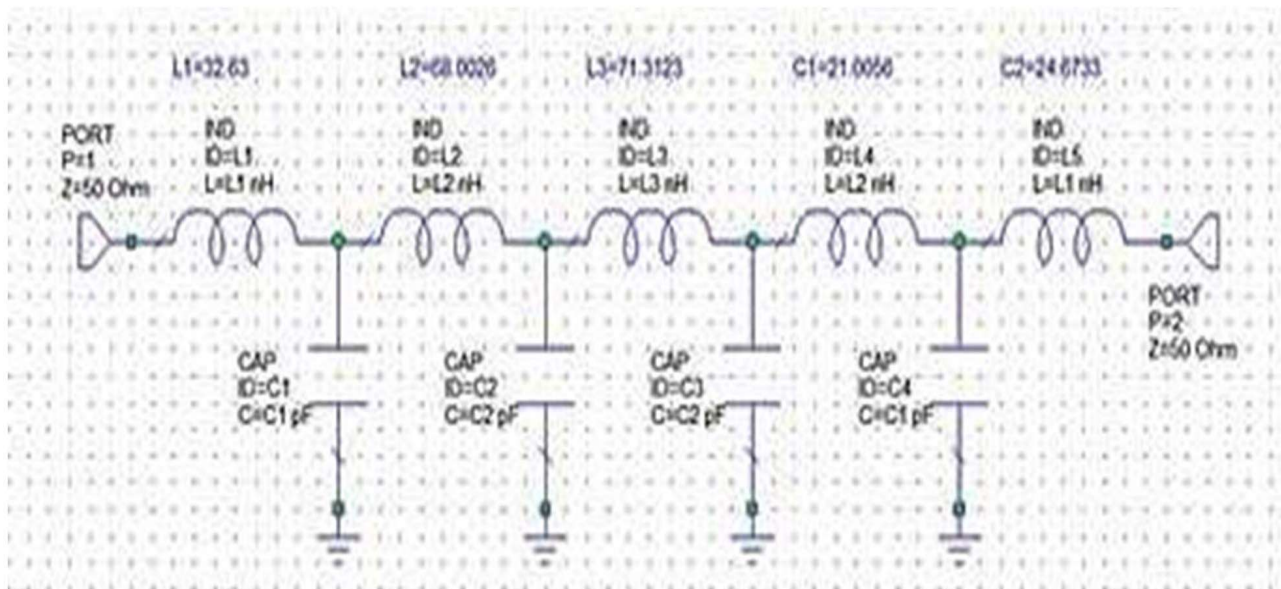


Figure 2. The schematic of the low pass filter circuit

During the filter realization, all the inductors were designed with the help of formula [3],

$$L = \frac{0.394r^2N^2}{9r+10l}, \quad (9)$$

where r is the coil radius in cm , l is the coil length in cm , N is the number of turns and L is the inductance in μH .

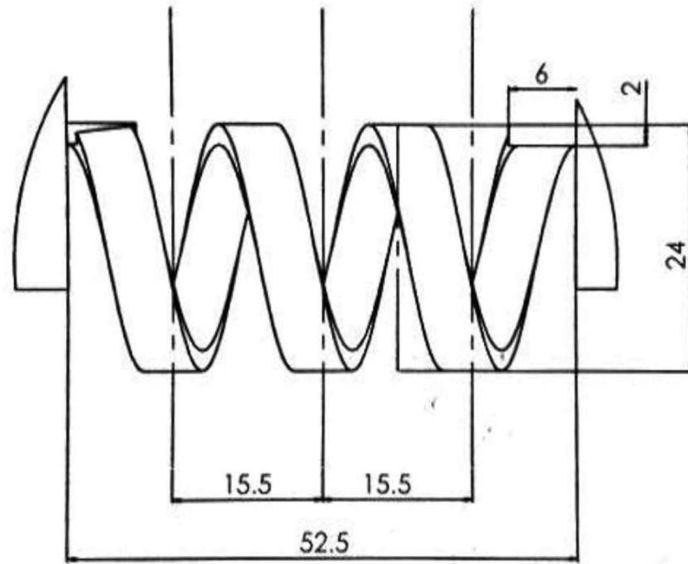


Figure 3. The schematic of a coil, with the inductance L_A

Every ideal inductor in Figure 2, with the inductance L_2 , was substituted with the coil in Figure 3, with the inductance L_A , in order to realize the filter. The coil in Figure 3, has three turns and was designed as a copper strip of thickness $t = 2$ mm, of radius $r = 10$ mm, of length $l = 52.5$ mm and of width $w = 6$ mm. The inductance of a coil in Figure 3, according to formula (9), is $L_A = 57.6585$ nH.

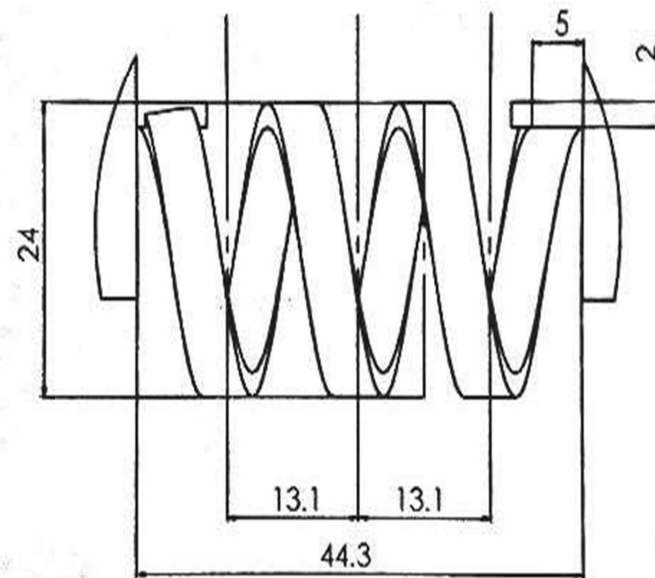


Figure 4. The schematic of a coil, with the inductance L_B

The ideal inductor in Figure 2, with the inductance L_3 , was substituted with the coil in Figure 4, with the inductance L_B , in order to realize the filter. The coil in Figure 4, has three turns and was designed as a copper strip of thickness $t = 2$ mm, of radius $r = 10$ mm, of length $l = 44.3$ mm and of width $w = 5$ mm. The inductance of a coil in Figure 4, according to formula (9), is $L_B = 66.5291$ nH.

Every ideal inductor in Figure 2, with the inductance L_1 , was substituted with the coil in Figure 5, with the inductance L_C , in order to realize the filter. The coil in Figure 5, has two turns and was designed as a copper strip of thickness $t = 2$ mm, of radius $r = 9$ mm, of length $l = 30.45$ mm and of width $w = 6$ mm. The inductance of a coil in Figure 5, according to formula (9), is $L_C = 33.1144$ nH. All the dimensions in Figures 3, 4 and 5 are in mm.

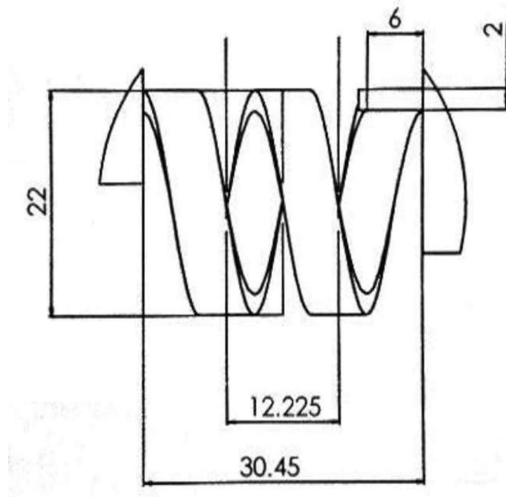


Figure 5. The schematic of a coil, with the inductance L_C

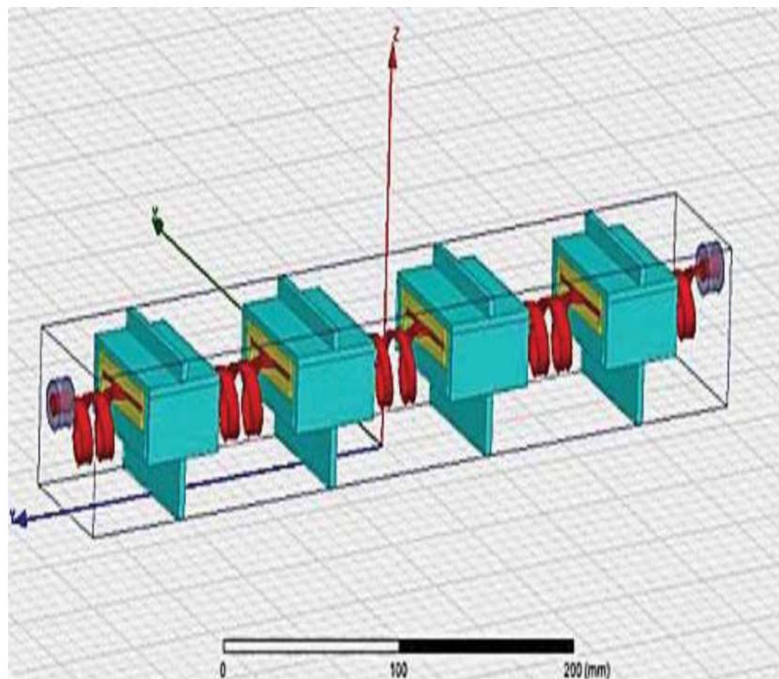


Figure 6. The isometric view of the model of the VHF low pass filter in 3D EM simulator

In Figure 6, looking from left to right, we can see the substitutions for the ideal capacitors C_1 and C_2 from Figure 2. Every ideal capacitor C_1 , in Figure 2, was substituted with the parallel connection of two capacitors, Figure 6, with the equivalent capacitance of $C_1 = 19.2281$ pF. Every ideal capacitor C_2 , in Figure 2, was substituted with the parallel connection of two capacitors, Figure 6, with the equivalent capacitance of $C_2 = 20.9374$ pF.

3. Simulation and Measurement Results

3.1. Simulation

Being aware of the criteria that our filter has to meet, the return loss, $-20 \log|S_{21}|$, larger than 20 dB, and the insertion loss, $-20 \log|S_{21}|$, smaller than 0.1 dB, for the frequency range from 150 MHz to 200 MHz, we were able to direct the process of 3D EM simulation towards satisfying the above-mentioned conditions and obtaining the final dimensions of the filter, shown in Figure 6. Frequencies below 150 MHz are of no interest to us because they were reduced or eliminated by previous filtering stages of the system. The inductors dimensions were firstly determined through the application of formula (9) and were later corrected through 3D EM simulation. The capacitors dimensions were firstly obtained through the application of a well-known formula for the capacitance of parallel-plate capacitors:

$$C = \epsilon_0 \epsilon_r \frac{S}{d} \quad (10)$$

where ϵ_0 is the vacuum permittivity, ϵ_r is the relative permittivity of the dielectric, S is the area of the plates, and d is the distance between the plates. In our case dielectric is Teflon, so $\epsilon_r = 2.1$. The capacitors dimensions were later corrected through 3D EM simulation. As we can see from Figure 7, capacitors in a parallel connection that form equivalent capacitor C_1 , share the same copper plate (colored in red), of the dimensions 45 mm x 46.2 mm x 2 mm, that is surrounded by Teflon in an aluminum housing. In Figure 7, Teflon is colored in yellow and aluminum is colored in blue.

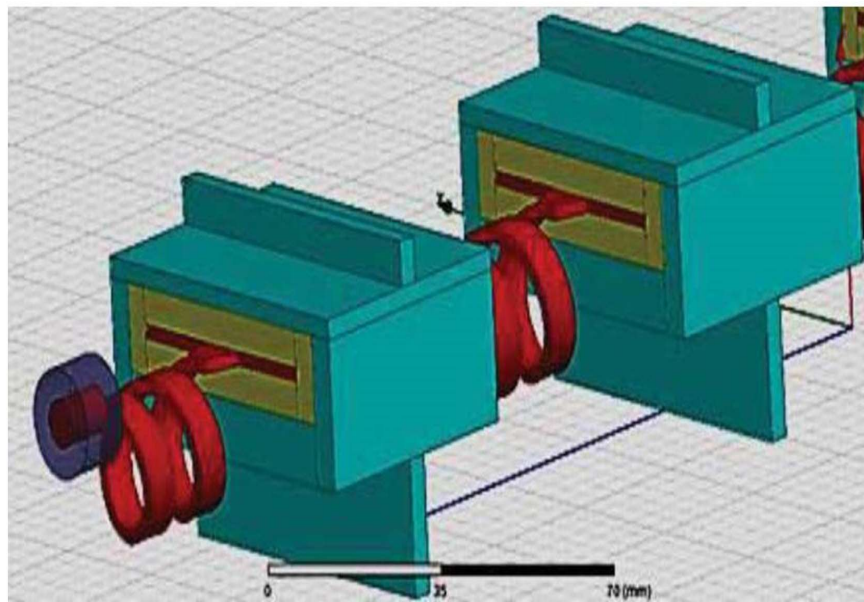


Figure 7. The model of the capacitors C_1 and C_2 in 3D EM simulator

As we can see from Figure 7, capacitors in a parallel connection that form equivalent capacitor C_2 , share the same copper plate (colored in red), of the dimensions 45 mm x 50.8 mm x 2 mm, that is surrounded by Teflon in an aluminum housing. The distance d between the plates, for capacitors in a parallel connection that form both C_1 and C_2 , is the same and equal to 5.45 mm. The photograph of the produced filter is given in Figure 8.



Figure 8. The produced VHF low pass filter

Because of the edge effect, the capacitances C'_1 and C'_2 were calculated using the Method of Moments. The inductors and the capacitors are placed in the aluminum casing, filled with air. The length of the casing is 404.2 mm, the height of the casing is 51.4 mm and the width of the casing is 65 mm. All the dimensions in Figure 9 are in mm.

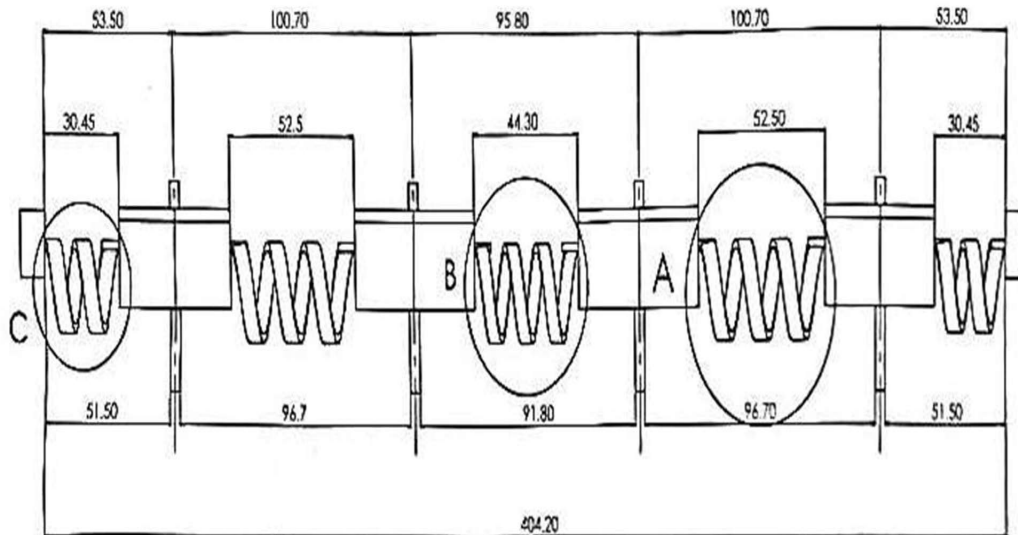


Figure 9. The schematic of the lateral dimensions of the VHF low pass filter

The filter uses two 7/16-connectors.

3.2. Simulated and Measured Results

As we can see from Figure 10, the return loss is larger than 21 dB in the frequency range from 150 MHz to 200 MHz, which is satisfactory. Unfortunately, the insertion loss exceeds 0.1 dB, in the same frequency range, due to losses in conductors and dielectric. The highest insertion loss in the frequency range of interest is 0.16 dB.

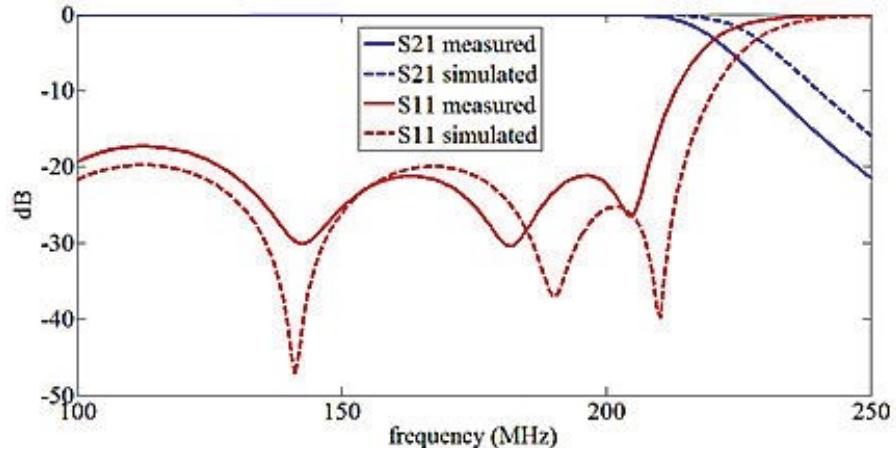


Figure 10. Comparison of simulated and measured magnitudes of S_{21} and S_{11}

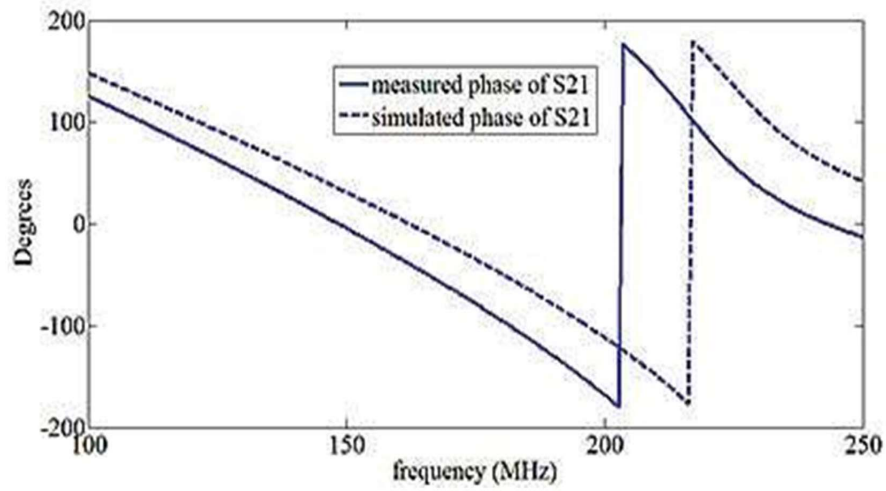


Figure 11. Comparison of simulated and measured phase angle of S_{21}

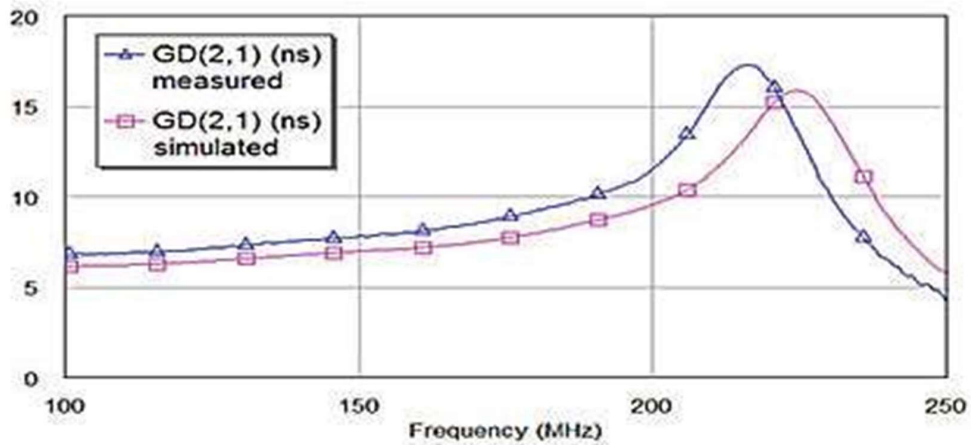


Figure 12. Comparison of simulated and measured group delay

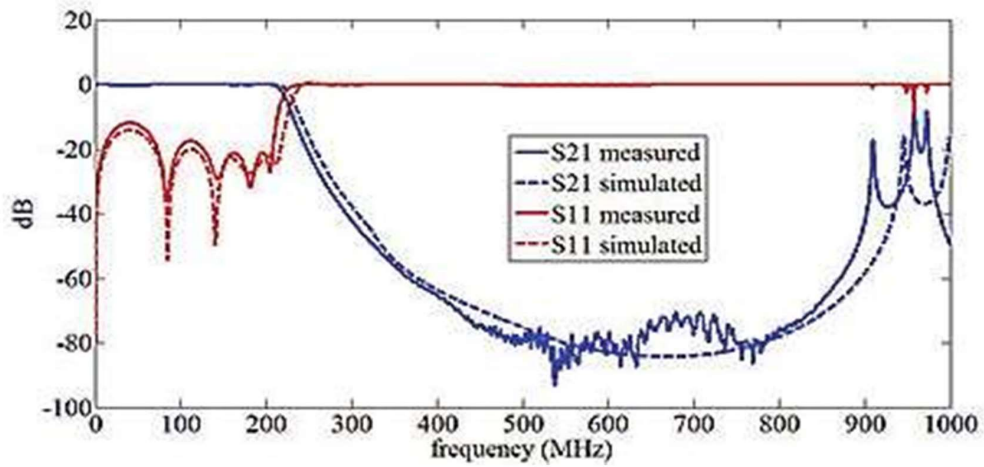


Figure 13. Comparison of simulated and measured magnitudes of S_{21} and S_{11}

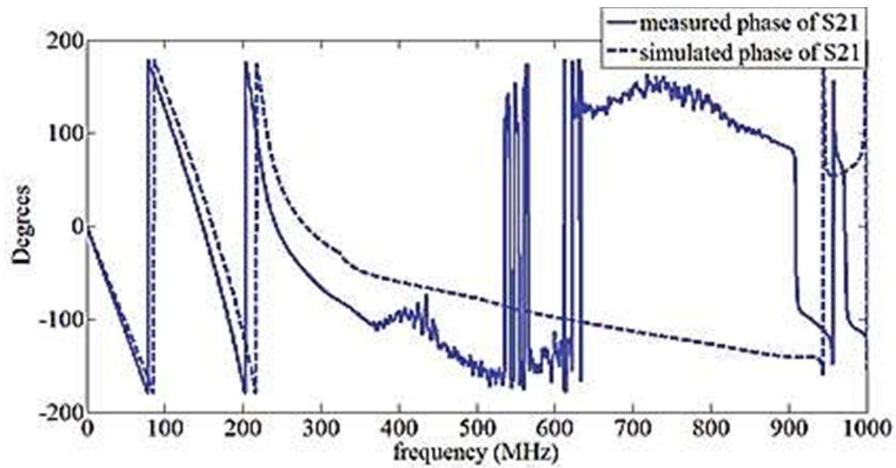


Figure 14. Comparison of simulated and measured phase angle of S_{21}

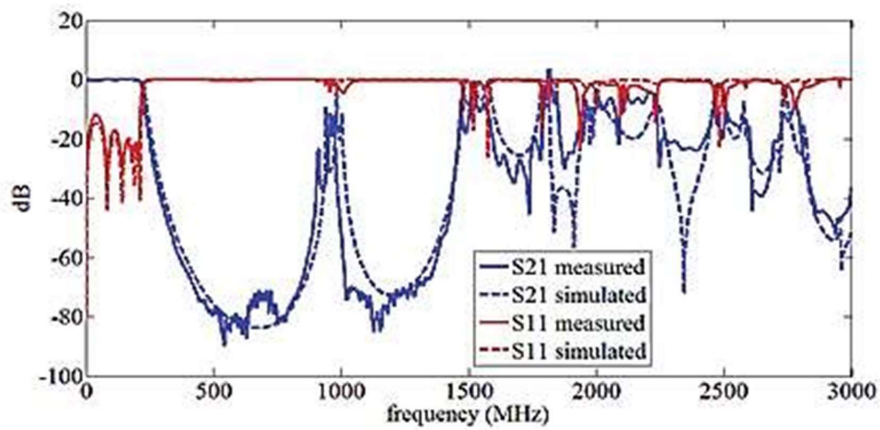


Figure 15. Comparison of simulated and measured magnitudes of S_{21} and S_{11}

It can be seen from Figure 11, that the phase response of the filter is nonlinear, which has for a consequence a nonconstant group delay, as it is shown in Figure 12.

These are all the typical traits of a Chebyshev low pass filter. Ideally, the filter is a lossless two-port network, which means that the zeros of the reflection coefficient are located at $k-1$ in the frequencies $f_k = f_c \cos \frac{(2k-1)\pi}{2N}$, that is $f_k = 0, 75.24\text{MHz}, 141.41\text{MHz}, 190.52\text{MHz},$ and 216.66MHz . We can see from Figure 13, that there are five zeros of the reflection coefficient and they are

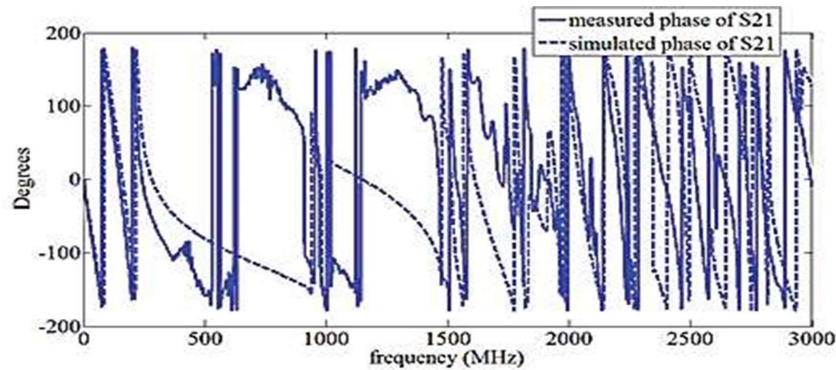


Figure 16. Comparison of simulated and measured phase angle of S_{21} and S_{11}

located around above-mentioned frequencies, which is the sign of good filter design. The insertion loss at 300 MHz is 42.01 dB, as it is shown in Figure 13. Nonlinearity of the filter phase response only increases with frequency, as can be seen in Figures 14 and 16. Real filters have re-entry modes that limit the high-frequency capability of the filter [4]. It can be seen in Figures 13 and 15, that higher frequency signals can appear at the output of the filter.

4. Conclusion

In this paper, we have thoroughly explained the theory behind and the design of the VHF Chebyshev low pass filter with lumped elements. Our primary objective was to design the low pass filter that can be used for high power applications, more precisely at the output of a high power amplifier, where it would reduce or eliminate harmonics. In such an application, the nonlinearity of the phase response is not important, the only thing that matters is that the transition between passband and stopband be sharp enough, so for that reason, the Chebyshev low pass response was chosen. The bulky dimensions of the filter are a consequence of the purpose for which the filter was built. The goals regarding the level of the return loss in the passband and the level of the insertion loss in the stopband were met. Only the level of the insertion loss in the passband has exceeded the projected value by a small margin, at the first place because of the losses introduced by real inductors, and at the second place because of the losses introduced by Teflon.

Acknowledgement

This paper was partially supported by the Ministry of Education, Science and Technological Development of the Republic of Serbia under grant TR-32024.

References

- [1] Kinayman, N., Aksun, M. I. (2005). Modern Microwave Circuits, 1st ed., ARTECH HOUSE, 2005, p 415-437.
- [2] Misra, D. K. (2001). Radio-Frequency and Microwave Communication Circuits, 1st ed., John Wiley & Sons, p. 322.
- [3] Bowick, C. RF Circuit Design, Newnes, 1997, p 17.
- [4] <https://www.markimicrowave.com/blog/engineering/resources/rf-and-microwave-knowledge-base/#filters>.